

ROBERT KOCH INSTITUT



Originally published as:

Thaa, B., Tiesch, C., Möller, L., Schmitt, A.O., Wolff, T., Bannert, N., Herrmann, A., Veit, M.
Growth of influenza A virus is not impeded by simultaneous removal of the cholesterol-binding and acylation sites in the M2 protein
(2012) Journal of General Virology, 93 (2), pp. X282-292.

DOI: 10.1099/vir.0.038554-0

This is an author manuscript that has been accepted for publication in Journal of General Virology, copyright Society for General Microbiology, but has not been copy-edited, formatted or proofed. Cite this article as appearing in Journal of General Virology. This version of the manuscript may not be duplicated or reproduced, other than for personal use or within the rule of 'Fair Use of Copyrighted Materials' (section 17, Title 17, US Code), without permission from the copyright owner, Society for General Microbiology. The Society for General Microbiology disclaims any responsibility or liability for errors or omissions in this version of the manuscript or in any version derived from it by any other parties. The final copy-edited, published article, which is the version of record, can be found at <http://vir.sgmjournals.org>, and is freely available without a subscription 12 months after publication.

Growth of influenza A virus is not impeded by simultaneous removal of the cholesterol binding and acylation sites in the M2 protein

Bastian Thaa (1), Claudia Tievesch (1), Lars Möller (2), Armin O. Schmitt (3[†]), Thorsten Wolff (2), Norbert Bannert (2), Andreas Herrmann (4), Michael Veit (1*)

(1): Freie Universität Berlin, Faculty of Veterinary Medicine, Institute of Immunology and Molecular Biology, Philippstraße 13, 10115 Berlin, Germany

(2): Robert Koch Institute, Nordufer 20, 13353 Berlin, Germany

(3): Humboldt-Universität zu Berlin, Department for Crop and Animal Sciences, Invalidenstraße 42, 10115 Berlin, Germany

(4): Humboldt-Universität zu Berlin, Institute of Biology, Molecular Biophysics, Invalidenstraße 42, 10115 Berlin, Germany

Word count:

Summary: 249 words, Text: 5479 words

Running title: Growth of influenza virus with mutated M2

([†]): present address: Faculty of Science and Technology, Free University of Bolzano/Bozen, Universitätsplatz 5/Piazza Università 5, 39100 Bozen/Bolzano, Italy

(*): corresponding author: mveit@zedat.fu-berlin.de

1 Summary

2 Influenza virus assembly and budding occur in the “budozone”, a coalesced raft domain in the
3 plasma membrane. The viral transmembrane protein M2 is implicated in virus particle scission,
4 the ultimate step in virus budding, probably by wedge-like insertion of an amphiphilic helix into
5 the membrane. In order to do so, M2 is hypothesised to be targeted to the edge of the budozone,
6 mediated by acylation and cholesterol binding.

7 We have recently shown that acylation and cholesterol binding affect membrane association of
8 M2’s cytoplasmic tail and targeting of the protein to coalesced rafts. In this study, we tested
9 whether the combined removal of the acylation site (C50) and the cholesterol-binding CRAC
10 motifs (key residues Y52, Y57) in M2’s amphiphilic helix influence virus formation.

11 We generated recombinant influenza viruses in the WSN background with mutations in one or
12 both of these features. All these viruses showed, in comparison with the wildtype, very similar
13 growth kinetics in various cell types. Wildtype and mutant viruses differed in their relative M2
14 content, but not regarding the major structural proteins. The morphology of the viruses was not
15 affected by mutating M2. Moreover, wildtype and mutant viruses showed comparable
16 competitive fitness in infected cells. Lastly, a global comparison of M2 sequences revealed that
17 there are natural virus strains with M2 devoid of both lipid-association motifs. Taken together,
18 acylation and cholesterol-binding motifs in M2 are not crucial for replication of influenza virus
19 in cell culture, indicating that also other factors can target M2 to the budding site.

20

1 Introduction

2 Influenza A viruses are heteromorphous (spherical or filamentous), enveloped viruses in the
3 family *Orthomyxoviridae*. Their membrane is lined from beneath by a matrix protein layer
4 composed of the protein M1, which in turn envelopes the viral genome, arranged as eight viral
5 ribonucleoprotein particles (vRNPs). The membrane contains three transmembrane proteins,
6 the glycoproteins haemagglutinin (HA) and neuraminidase (NA) and the tetrameric proton
7 channel protein M2. M2 (**Fig. 1a**) comprises 97 amino acid residues/monomer, with the N-
8 terminal 24 residues oriented towards the outside (ectodomain). The next 19 residues form a
9 transmembrane domain assembled into a four-helix bundle that constitutes the proton channel.
10 The residues 44–97 of M2 represent the cytoplasmic tail (M2-CT). Residues 48–62 form a
11 membrane-parallel amphiphilic helix with a hydrophilic (solvent-exposed) and a hydrophobic
12 (partially membrane-inserted) side. In addition, the M2-CT contains a binding site for M1
13 (residues 71–73, (Chen *et al.*, 2008)).

14 In the infected cell, all these components are synthesised and ultimately transported to the
15 apical plasma membrane for assembly and budding of progeny virions (Nayak *et al.*, 2009;
16 Rossman & Lamb, 2011). Assembly is organised in “membrane rafts”, cholesterol- and
17 sphingolipid-enriched nanodomains in the apical plasma membrane. These rafts are stabilized
18 to form the “viral budozone” mainly by interactions among the viral components and with the
19 raft lipids. The glycoproteins HA and NA have intrinsic raft-association features (Engel *et al.*,
20 2010; Scheiffele *et al.*, 1997; Scolari *et al.*, 2009) and hence define the site of the budozone
21 ((Hess *et al.*, 2005; Leser & Lamb, 2005), reviewed in (Veit & Thaa, 2011)). Conversely, the third
22 transmembrane protein, M2, does not associate with typical raft markers (Leser & Lamb, 2005;
23 Schroeder *et al.*, 2005; Thaa *et al.*, 2010; Zhang *et al.*, 2000) and is, accordingly, mostly excluded
24 from virions, although the protein is highly expressed at the infected cell’s surface (Lamb *et al.*,
25 1985). Still, some of the M2 molecules need to reach the budozone for inclusion into virions.

26 Targeting to the budozone might be achieved by the amphiphilic helix in the M2-CT, which
27 comprises two potential raft-association features: (1) S-acylation (“palmitoylation”: covalent
28 attachment of a saturated fatty acid, usually palmitic acid, by thioester linkage) at cysteine
29 residue 50 (Sugrue *et al.*, 1990; Veit *et al.*, 1991), and (2) cholesterol binding (Schroeder *et al.*,
30 2005), most likely mediated by cholesterol recognition/interaction amino acid consensus
31 (CRAC) motifs (L/V-X₁₋₅-Y-X₁₋₅-R/K), present up to four times in the amphiphilic helix region of
32 the M2-CT depending on the virus strain. Schroeder *et al.* have hypothesised that M2 could
33 accumulate at the edge of raft domains because the transmembrane domain is too short to be
34 completely immersed in the highly-ordered raft phase and thus counteracts the raft-targeting
35 features. Positioning of M2 at the raft edge could then entail the scission of virus particles: the

1 amphiphilic helix is assumed to induce curvature by wedge-like integration into the membrane
2 (Schroeder *et al.*, 2005). Indeed, there is experimental evidence that M2 plays an active role in
3 scission. M2 accumulates at the neck of budding filamentous virions (the budzone edge), and
4 M2 as well as a peptide encompassing the amphiphilic helix induce the formation of vesicles in
5 giant unilamellar vesicles (GUVs), an *in vitro* membrane model system (Rossman *et al.*, 2010a;
6 Rossman *et al.*, 2010b).

7 We recently demonstrated that M2 intrinsically meets biochemical requirements of the
8 Schroeder model: Mutation of tyrosines 52 and 57 (as part of overlapping CRAC motifs)
9 abrogates cholesterol binding to M2-CT as purified protein. Furthermore, we showed that M2-
10 CT associates with membranes, both *in vitro* and in cells, and that the membrane-binding
11 properties are modulated by exchange of the acylation site and the CRAC motif tyrosines.
12 Furthermore, M2 has the propensity to partly associate with the coalesced raft phase in cell-
13 derived model membranes, dependent on acylation (Thaa *et al.*, 2011).

14 Here we have tested whether the same mutations in M2's amphiphilic helix influence the growth
15 properties of recombinant virus. Others have reported previously that mutations in either the
16 acylation site or in the CRAC motifs of M2 do not significantly affect virus growth, at least in cell
17 culture (Castrucci *et al.*, 1997; Grantham *et al.*, 2009; Rossman *et al.*, 2010a; Stewart *et al.*, 2010).
18 However, the combined replacement of the two raft-association features in the amphiphilic helix
19 of M2 has not been investigated so far in the context of the virus. Our hypothesis was that the
20 *combined* elimination of both features would disconnect M2 from the budzone, leading to
21 impeded virus budding. However, our results show that virus replication in cell culture is not
22 markedly compromised by mutating one or both raft-targeting features in M2. This finding is
23 discussed with focus on molecular interactions and functional redundancy of influenza virus
24 proteins.

25

1 Results

2 *Generation of recombinant virus and growth kinetics*

3 In **Figure 1b**, the amphiphilic helix of influenza A virus M2 is displayed as a “helical wheel plot”.
4 This view along the helix axis shows the position of the individual amino acid residues; the helix
5 is amphiphilic since charged/hydrophilic residues (dark grey) are clustered at one side of the
6 helix and hydrophobic residues (light grey) at the other, directed towards the membrane. This
7 has also been verified experimentally (Nguyen *et al.*, 2008; Sharma *et al.*, 2010).

8 In previous studies, the acylation site cysteine 50 (see **Fig. 1c**, (Castrucci *et al.*, 1997; Grantham
9 *et al.*, 2009)) or up to three residues in the CRAC motifs (**Fig. 1d**, (Stewart *et al.*, 2010)) were
10 replaced in the background of the strain Influenza A/WSN/33 (H1N1) as well as A/Udorn/72
11 (H3N2), albeit without noticeable influence on viral replication in cell culture compared to the
12 respective wildtype. Note that in the Udorn M2, the CRAC motif sequence consensus (L/V-X₁₋₅-Y-
13 X₁₋₅-R/K) is not present. However, the protein associates with cholesterol (Rossman *et al.*,
14 2010a), and the completion of the CRAC motif does not alter viral growth (Stewart *et al.*, 2010).
15 To provoke a marked reduction in virus viability, five residues in the hydrophobic face of the
16 amphiphilic helix had to be replaced in Udorn M2 (**Fig. 1e** (Rossman *et al.*, 2010a; Rossman *et*
17 *al.*, 2010b)). However, none of these investigations examined the effects of a combined mutation
18 of the acylation site and the CRAC motifs on influenza virus growth.

19 To this end, we produced three different recombinant viruses encoding M2 mutations in the
20 WSN background (see **Fig. 1b**): In the mutant WSN M2: Y52S, Y57S, the CRAC motifs were
21 interrupted by replacing the two central tyrosine residues by serines, a mutation shown to
22 abrogate cholesterol binding to purified M2-CT without changing the hydrophobicity pattern of
23 the amphiphilic helix, and not to reduce acylation (Thaa *et al.*, 2011). In WSN M2: C50S, the
24 acylation site cysteine 50 was substituted by serine, and in the mutant WSN M2: C50S, Y52S,
25 Y57S, the two features were disrupted simultaneously.

26 All viruses could be rescued, as evidenced by plaque assay (**Fig. 2a**). Overall, the plaque size did
27 not differ significantly between wildtype and mutants, implying that the mutants do not exhibit
28 drastic growth defects. The mutant viruses could be passaged three times in Madin–Darby
29 canine kidney (MDCK) cells without changes in the M2 sequence showing that the respective
30 mutation was stable (data not shown).

31 To analyse replication kinetics of the viruses, MDCK cells were infected with WSN wildtype or
32 one of the mutants at a multiplicity of infection (MOI) of 0.01, supernatants were collected at
33 various times and assessed for virus titre by plaque assay (**Fig. 2b**). The mutant with deleted
34 acylation site reached identical titres as the wildtype virus confirming data by others for WSN as
35 well as Udorn (Grantham *et al.*, 2009). The mutant M2: Y52S, Y57S revealed reduced titres at 16

1 and 24 hours post-infection, albeit by less than one order of magnitude. Yet, this virus reached
2 the same titres as wildtype at later times, showing that any possible delay in growth is not long-
3 lasting. This is in line with investigations where similar mutations in M2's CRAC motifs did not
4 perturb the growth of WSN either (Stewart *et al.*, 2010).
5 Surprisingly, the mutant lacking both the acylation site and the CRAC motifs (C50S, Y52S, Y57S)
6 did not exhibit any reduction in titre at any time.
7 We next analysed viral growth kinetics on cell types derived from the actual target organ of
8 influenza virus, the respiratory tract. In the human alveolar epithelial adenocarcinoma cell line
9 A549, the virus grew to titres that were generally lower compared to those in MDCK cells, but
10 the growth kinetics were essentially identical for wildtype and mutant WSN (**Fig. 2c**). Likewise,
11 all M2 mutant viruses also replicated comparably to wildtype in non-transformed MRC-5
12 human foetal lung fibroblasts (Jacobs *et al.*, 1970) that can be regarded as primary cells (**Fig.**
13 **2d**). Similarly to the situation in MDCK cells (**Fig. 2b**), there was a 10-fold reduction in virus titre
14 for the M2: Y52S, Y57S mutant at intermediate (48 hours post-infection), but not at later times.
15 The additional replacement of C50 did not intensify this effect as the mutant WSN M2: C50S,
16 Y52S, Y57S grew identically as wildtype. Taken together, the mutation of the acylation site in
17 combination with the CRAC motifs in M2 did not perturb replication of WSN in different cell
18 systems. The mutant viruses characterised in this study may, however, be attenuated in animal
19 hosts, e.g. mice. Indeed, such findings were reported both for viruses where the acylated
20 cysteine in M2 was replaced (Grantham *et al.*, 2009) and where the CRAC motifs were disrupted
21 (Stewart *et al.*, 2010).

22

23 *Electron microscopy*

24 Defects in budding and scission might be reflected by aberrant morphology of the resulting virus
25 particles (Nayak *et al.*, 2009). This was the case when five residues in the hydrophobic face of
26 M2's amphiphilic helix were replaced in the filamentous Udorn strain (Rossman *et al.*, 2010a).
27 To examine whether acylation and/or the cholesterol-binding moiety of M2 have an influence on
28 virion shape, particles were harvested from the supernatant of infected MDCK cells and
29 visualised by negative-stain transmission electron microscopy. **Fig. 3a** shows that the virus
30 particles were mostly spherical in all cases, yielding no evidence for any perturbation of virus
31 morphology by mutations in M2. In addition, ultrathin sections of infected cells were produced
32 and imaged by transmission electron microscopy. Defects in the last budding step (scission)
33 would be reflected by a "beads-on-a-string" morphology of the budding virions, in which
34 individual virions fail to be separated from each other (Nayak *et al.*, 2009). Despite scrutinised
35 inspection of samples, no such morphology was observed. The representative images in **Fig. 3b**
36 show MDCK cells with WSN M2: Y52S, Y57S in the process of budding. This was the only mutant

1 that exhibited a slight reduction in titres (see **Fig. 2b/d**). Thus, WSN virus morphology is not
2 altered by mutating the acylation site and/or the CRAC motifs in M2's amphiphilic helix.

3 *Viral protein content*

4 We then assessed the content of the individual virus components in virus particles. If there was
5 an influence of the raft-targeting motifs in M2 on the incorporation of viral proteins, there
6 should be a difference in their relative abundance. However, the proportion of the major
7 structural proteins, especially the ratio HA/M1, was the same in WSN wildtype and the mutants
8 as illustrated with radioactively labelled virions by SDS-PAGE, fluorography and densitometric
9 quantification (**Fig 4a**). This is in line with other reports investigating similar mutations
10 (Grantham *et al.*, 2009; Rossman *et al.*, 2010a; Stewart *et al.*, 2010).

11 M2 cannot be discerned in the fluorograms in **Fig. 4a** since only minor amounts are
12 incorporated into virions. Therefore, Western blot with an anti-M2 antibody was performed
13 (**Fig. 4b**). The chemiluminescent signal intensity for M2 was related to that of M1 probed on the
14 same membrane in parallel. M2 was detected as a double-band as noticed previously (Grantham
15 *et al.*, 2009; Zhirnov *et al.*, 1999). In comparison to wildtype, WSN M2: Y52S, Y57S showed a
16 significantly reduced M2/M1 ratio (i.e., less M2 incorporation). The mutant WSN M2: C50S, in
17 contrast, contained more than twice the amount of M2 (normalised to M1) than wildtype.
18 Interestingly, the virus in which both the cholesterol-association motifs and the acylation site
19 were disrupted (WSN M2: C50S, Y52S, Y57S) did not display any marked change in the M2/M1
20 ratio compared to wildtype. Thus, the opposing effects of CRAC and acylation site mutation on
21 M2 integration into virions appear to compensate each other.

22 *Competition of wildtype and mutant virus*

23 We then hypothesised that mutating M2 might reduce the competitive fitness of the virus
24 compared to wildtype. If one of the virus strains exhibits a selective advantage, it would rapidly
25 eliminate the other. To test this, we co-infected MDCK cells with WSN wildtype and WSN M2:
26 Y52S, Y57S (the mutant showing slight growth retardation) and analysed the cell culture
27 supernatant after different times. The viral RNA in the supernatant was isolated, reverse-
28 transcribed into copy-DNA (cDNA), PCR-amplified and sequenced. **Fig. 5a** shows the sequencing
29 chromatograms for the region of interest in the M2 gene in WSN wt and WSN M2: Y52S, Y57S
30 (mut). When the supernatants of cells co-infected with wt and mut viruses (at a ratio of 1:1 or
31 1:5; total MOI = 0.005) were analysed by sequencing, the two nucleotide species (wt and mut)
32 were present in all cases, reflected by superimposed peaks for the respective bases (marked
33 with arrows) in **Fig. 5b** (wt:mut = 1:1) and **Fig. 5c** (wt:mut = 1:5). Note that differences in peak
34 heights and areas in the chromatograms should not be interpreted in a precise quantitative
35 manner. Nevertheless, it is obvious that the mutant did not become "extinct" within the

1 timeframe of the experiment (96 hours). Competition experiments involving WSN wt and the
2 other mutant viruses yielded the same result (data not shown).
3 This is in contrast to recombinant viruses where the M2 proton channel is inactivated by the
4 deletion of three amino acids in the transmembrane domain. In that case an analogous fitness
5 assay revealed that wildtype virus almost completely overgrows the mutant virus within
6 96 hours of co-cultivation even if the initial amount of wildtype is much lower (ratio wt:mut =
7 1:100) (Takeda *et al.*, 2002). Thus, our result demonstrates that there is no considerable
8 decrease in viral fitness upon disruption of M2's raft-targeting features.

9 *Conservation of acylation site and CRAC motifs in influenza A virus M2 protein*

10 Surprisingly, our combined experimental evidence argues against a synergistic role of M2's
11 acylation site C50 and the CRAC motif tyrosines for virus viability in cell culture. However, it has
12 been noted that neither C50 (Sugrue *et al.*, 1990; Veit *et al.*, 1991) nor the CRAC motifs (e.g. in
13 the Udorn strain) are strictly conserved in M2, implying that these features are not absolutely
14 essential for virus replication.

15 To find out whether there are also natural influenza virus strains in which both C50 *and* CRAC
16 are absent (like in WSN M2: C50S, Y52S, Y57S), we analysed a total number of 18,477 influenza
17 A M2 sequences retrieved from www.ncbi.nlm.nih.gov comprising at least 40 amino acids and
18 containing residue 50. Multiple alignment of these sequences and bioinformatic data-mining
19 revealed that a vast majority (84.0 %) of all deposited M2 sequences contain both a cysteine as
20 residue 50 and at least one intact CRAC motif (see **Table 1** for results). In 13.8 % of all
21 sequences, CRAC is preserved, but C50 is replaced by another amino acid: Serine at position 50
22 is observed mostly in human H1N1 strains; phenylalanine is present mainly in sequences of
23 equine and canine H3N8 viruses, but also in human and chicken H5N1 strains; and tyrosine is
24 found in bird strains, mainly of H6 subtype. Phenylalanine and tyrosine are bulky aromatic
25 residues with relatively high hydrophobicity and membrane-insertion capacity. Thus they might
26 at least partially compensate for the hydrophobicity of the wildtype S-acylated cysteine,
27 contrary to serine with its hydrophilic hydroxyl group.

28 1.9 % of all M2 sequences analysed possess C50 but no CRAC motif. These are mainly sequences
29 from H3N2 viruses of human, porcine or avian origin, including the pandemic strain of the 1968
30 outbreak (A/Aichi/2/68) and the filamentous laboratory strain Udorn. The M2 of these viruses
31 might, however, still be capable of binding cholesterol, possibly with decreased affinity. The
32 CRAC motif is defined rather loosely (L/V-X₁₋₅-Y-X₁₋₅-R/K) and probably depends on protein
33 conformation rather than just the linear amino acid sequence (Schroeder, 2010). One of the two
34 tyrosines demonstrated to be important for cholesterol association (Thaa *et al.*, 2011) is usually
35 present in these strains.

36 Lastly, a total number of 58 sequences (0.3 %) lack both the acylated cysteine at position 50 and

1 an intact CRAC motif. Of these, 12 sequences are artificial (sequences of M2 fragments for
2 structural analysis), and the M2 sequence of one particular strain (A/Sendai/TU65/2006
3 (H1N1)) was deposited at the database seven times. Notably, four of these strains carry a
4 cysteine at position 52, which can be assumed to be a potential acylation site instead of the
5 natural C50. Thus, there are 36 different, naturally occurring influenza A virus strains in the
6 database whose M2 lack both acylation and cholesterol-binding motifs. This proves that such
7 mutants indeed exist in nature. These strains are mostly human isolates from different
8 geographic regions (Asia, Europe, America) typically isolated in 2000 or later and exclusively of
9 subtype H1N1. It will be interesting to see whether new strains with these features will emerge;
10 the result from our competition experiment (**Fig. 5**) is a hint that such mutants are not quickly
11 competed out by wildtype.

12 In summary, this global sequence comparison shows that the “standard” M2 protein contains
13 both a palmitoylated cysteine at position 50 and at least one intact CRAC motif in the
14 amphiphilic helix. However, there are strains in which one or even both of these features are
15 missing.

16

1 Discussion

2 Our experimental data collectively show that the combined disruption of the acylation site and
3 the CRAC motifs in M2's amphiphilic helix has no effect on virus viability in cell culture although
4 these features determine the membrane association capacity of the M2-CT and, in the case of
5 acylation, also the partial association of M2 with coalesced rafts in giant plasma membrane
6 vesicles, cell-derived model membranes (Thaa *et al.*, 2011). Yet, an effect on incorporation of
7 mutated M2 into virus particles was observed. Hence, we assume that targeting to the viral
8 budzone was modified after disruption of CRAC and the acylation site, but did not result in
9 diminished virus growth.

10 Although cholesterol binding to the purified M2-CT (determined by crosslinking with [³H]-
11 photocholesterol) is drastically reduced upon mutation of the CRAC motif tyrosines (Thaa *et al.*,
12 2011), we do not want to exclude that M2: Y52S, Y57S expressed during influenza virus infection
13 has residual cholesterol binding activity that may be critical to virus growth. It can be imagined
14 that M2's transmembrane region contributes to cholesterol binding. Moreover, the cholesterol
15 concentration in the plasma membrane and especially at the viral budzone might be high
16 enough to allow association with even mutated M2. Technical limitations to label M2 and even
17 the established cholesterol-binding protein caveolin ((Murata *et al.*, 1995) and data not shown)
18 with [³H]-photocholesterol inside cells precluded our attempts to investigate this important
19 issue further. Likewise, the methods we have used previously to examine raft-localisation of M2,
20 namely FLIM-FRET (Thaa *et al.*, 2010) and the preparation of giant plasma membrane vesicles
21 (Thaa *et al.*, 2011), cannot be performed in the context of virus-infected cells.

22 Mutating C50 and/or CRAC in M2 did not impede virus replication. Yet we observed a reduced
23 incorporation of M2 into virions upon CRAC disruption, which corresponded with a slight delay
24 in virus replication. This might be due to a weaker interaction of the mutated M2 protein with
25 the cholesterol-rich budzone. In contrast, replacement of C50 led to an increased proportion of
26 M2 in the mature virions. The fatty acyl chains of palmitoylated proteins have been proposed to
27 tilt transmembrane helices relative to the bilayer normal and hence reduce their effective length.
28 Thus, lack of acylation might increase the interaction of M2 with raft domains (and hence the
29 viral budzones), which are considered to be thicker than the bulk phase of the plasma
30 membrane (Charollais & Van Der Goot, 2009; Morozova & Weiss, 2010). The virus in which both
31 the cholesterol-association motifs and the acylation site were disrupted did not display any
32 marked change in the M2/M1 ratio compared to wildtype. Hence, the opposing effects of CRAC
33 and acylation site mutation on the incorporation of M2 into virus particles apparently
34 compensate each other. Yet, the overall amount of M2 in mature virions is generally very low

1 (14–68 M2 molecules/virion), although the protein is abundantly expressed at the plasma
2 membrane (Zebedee & Lamb, 1988).

3 So far, only one mutation in M2's amphiphilic helix has been described to lead to an impairment
4 of virus growth in cells, namely the simultaneous replacement of five amino acids (F47, F48, I51,
5 Y52, F55) in the hydrophobic face of the helix by less hydrophobic alanines ((Rossman *et al.*,
6 2010a; Rossman *et al.*, 2010b), see **Fig. 1e**). However, this set of mutations severely reduces the
7 hydrophobic moment μ_H , a measure of the amphiphilicity of the helix (Eisenberg *et al.*, 1984).
8 The μ_H value is reduced from 0.502 in the wildtype case to 0.244. Note however that the
9 additional hydrophobicity of the cysteine-bound palmitate is not considered in this calculation.

10 In contrast, all other mutations that were engineered in the amphiphilic helix of M2, in this study
11 and those of others, do not markedly change the hydrophobic moment of the helix (listed in
12 **Table 2**). Concomitantly, viruses carrying these mutations in their M2 show similar growth
13 properties as wildtype. Thus, virus growth seems to depend rather on the amphiphilicity of the
14 helix in the M2-CT than on the presence or absence of the two potential raft-targeting features,
15 acylation and cholesterol association. We assume that the deepness of membrane insertion
16 exerted by the amphiphilic helix determines whether M2 can fulfil its suggested role as mediator
17 of virus particle scission.

18 This conclusion is further backed by a new report, published during revision of this manuscript
19 (Stewart & Pekosz, 2011). In that study, alanine scanning mutagenesis in M2's amphiphilic helix
20 did not markedly affect virus composition and viability, implying that this region tolerates
21 numerous mutations and that the functionality of M2 for virus formation is based on the overall
22 structure of the amphiphilic helix rather than its protein sequence.

23 The targeting failures of mutant M2, which we have observed for individually expressed M2
24 (Thaa *et al.*, 2011), is probably compensated for by interactions of M2 in the context of infection.
25 Most importantly, M2 binds to the viral matrix protein M1 via residues 71–73 in the M2-CT,
26 which are not situated within the amphiphilic helix (Chen *et al.*, 2008; McCown & Pekosz, 2006).
27 M1 is assumed to organise virus assembly by interactions with the other viral components,
28 including the cytoplasmic tails of raft-embedded HA and NA (Nayak *et al.*, 2009). M1 might thus
29 drag M2 to the edge of the budzone, even if the intrinsic budzone-targeting features in M2 are
30 disrupted. Accordingly, replacement of the acylation site and the CRAC motifs in M2 does not
31 reduce virus viability in cells, but mutating the M1 binding site in M2 does (Chen *et al.*, 2008).

32 It is the cooperative function of all the components that governs budzone organisation, virus
33 assembly and budding. Our results, showing that virus growth is not affected by the mutation of
34 the two lipid-interaction features in M2's amphiphilic helix, reinforce the notion that these
35 processes are very robust and partly redundant in their functionalities.

1 Methods

2 ***Cells***

3 MDCK II (ATCC CRL-2936), HEK-293T (ATCC CRL-11268), A 549 (ATCC CCL-185) and MRC-5
4 (ATCC CCL-171) cells were cultured in Dulbecco's modified Eagle's medium (DMEM, PAN
5 Biotech) supplemented with 10 % foetal bovine serum (FBS, Perbio) at 37 °C, 5 % CO₂, 95 %
6 humidity, using standard techniques.

7 ***Generation of recombinant virus***

8 Recombinant influenza A/WSN/33 (H1N1) virus was generated using the eight-plasmid reverse
9 genetics system (Hoffmann *et al.*, 2000), where each plasmid contains cDNA of one viral RNA
10 segment, flanked by suitable promoters. In the M1-/M2-encoding cDNA segment 7, the codons
11 for C50 (TGC) and/or Y52/Y57 (TAT/TAC) were replaced by serine codons (TCA, TCT and TCC,
12 respectively), using QuikChange mutagenesis (Stratagene), and checked by sequencing (GATC).
13 293T cells in 60-mm dishes were transfected with eight plasmids encoding WSN cDNA (1 µg
14 each) using TurboFect (Fermentas/Thermo) in OptiMEM medium (Invitrogen). 4–6 h after
15 transfection, medium was replaced by infection medium (DMEM + 0.2 % bovine serum albumin
16 + 0.1 % FBS + 2 mM glutamine + 1 µg/mL TPCK-treated trypsin (Sigma-Aldrich)) and incubation
17 was continued at 37 °C. 48 h after transfection, supernatants were harvested and cleared of
18 debris by low-speed centrifugation (2,000× g, 5 min, 4 °C). This supernatant was used to infect
19 MDCK cells for virus propagation. After 1 h of adsorption, cells were washed with phosphate-
20 buffered saline (PBS), infection medium was supplied and incubation was continued until
21 cytopathic effect became evident; then, the supernatant was harvested.

22 ***Growth curve***

23 To assess growth kinetics, cells were infected with recombinant WSN at a multiplicity of
24 infection (MOI) of 0.01. After 1 h of adsorption and washing with PBS, infection medium was
25 supplied. The supernatant was harvested after a defined incubation time, cleared of debris and
26 stored at –80 °C before titre determination by plaque assay.

27 ***Plaque assay***

28 Plaque assay was performed on MDCK cells in 6-well plates according to standard procedures.
29 Briefly, cells were infected with serial 10-fold dilutions of the virus supernatants in infection
30 medium, incubated for 1 h at 37 °C, washed with PBS and overlaid with 0.9 % SeaKem
31 agarose (Lonza) in Eagle's minimum essential medium (EMEM) supplemented with 0.2 %
32 bovine serum albumin, 0.1 % FBS, 2 mM glutamine, and 1 µg/mL TPCK-treated trypsin. After 3–

1 4 days of incubation, cells were stained using neutral red (0.02 % in PBS, Biochrom), and
2 plaques were counted.

3 ***Reverse transcription (RT)-PCR and sequencing***

4 To check for correctness of M2 sequences in the recombinant viruses, RNA was isolated from
5 cell culture supernatants with Invisorb Spin Virus RNA Mini Kit (Invitex) followed by reverse-
6 transcription and polymerase chain reaction (RT-PCR) using M2-specific primers and OneStep
7 RT-PCR kit (Qiagen). PCR products were purified from agarose gels using the Fragment CleanUp
8 Kit (Invitex) and sequenced (GATC).

9 ***Radioactive labelling of viruses, SDS-PAGE and Western blot***

10 Radioactively labelled virus particles were produced by infecting MDCK cells in a 15-cm dish at
11 MOI = 20. Three hours after infection, medium was replaced by DMEM lacking methionine,
12 cysteine and glutamine, supplemented with 0.2 % bovine serum albumin, 0.1 % FBS, 5 mM
13 glutamine, 1 µg/mL TPCK-treated trypsin and 0.3 µCi/mL [³⁵S]-methionine/-cysteine (Tran35S-
14 Label, MP Biomedicals). 24 h after infection, supernatants were harvested, cell debris was
15 removed (1,500× g, 10 min, 4 °C), and virus was pelleted from the supernatant by
16 ultracentrifugation (Beckman SW-28 rotor, 28,000 rpm, 2 h, 4 °C), resuspended in 100 µL PBS
17 and analysed by SDS-PAGE under reducing conditions and fluorography as described (Veit *et al.*,
18 2008), or by SDS-PAGE followed by Western blot using the monoclonal anti-M2 antibody 14C2
19 (Santa Cruz) and a polyclonal antiserum against fowl plague virus, which crossreacts with WSN-
20 M1, and horseradish peroxidase (HRP)-coupled secondary antibodies for chemiluminescence
21 detection using ECL plus substrate (GE Healthcare) and a Fusion SL camera system (Promega),
22 which detects photons over a wide linear signal-response range. Densitometric quantifications
23 were done with Bio-1D software (Vilmer-Lourmat).

24 ***Electron microscopy***

25 For negative staining, virus particles were pelleted from the supernatants of infected MDCK cells
26 as described for radioactive labelling of viruses. In each case 4 µl of the resulting virus
27 suspension were applied directly onto a carbon-coated, glow-discharged grid. After 10 min of
28 incubation grids were washed three times with bidistilled water and stained with uranyl acetate
29 (1 % in bidistilled water).

30 For ultrathin sections, MDCK cells were infected at an MOI of 100, fixed 8 h post-infection with
31 glutaraldehyde (2.5 % in 50 mM HEPES, pH 7.2) for 16 h at 4 °C and harvested by scraping. Cells
32 were centrifuged (2,000× g, 5 min, 4 °C) and resuspended in 2.5 % glutaraldehyde buffer. After
33 washing in 50 mM HEPES, pH 7.2, pellets were embedded in low melting-point agarose (3 % in
34 bidistilled water, 1:1). Cells were post-fixed with osmium tetroxide (1 % in bidistilled water,

1 1 h), tannic acid (0.1 % in 50 mM HEPES, pH 7.2, 30 min) and uranyl acetate (2 % in distilled
2 water, 2 h), dehydrated stepwise in a graded ethanol series and embedded in epon resin. Thin
3 sections (approx. 60 nm) were prepared with an ultramicrotome (Leica Ultracut UCT), and
4 counterstained with uranyl acetate (2 % in bidistilled water, 20 min.), followed by lead citrate
5 (Reynolds solution, 3 min.).

6 Negative stained samples and ultrathin sections were examined using a JEM-2100 transmission
7 electron microscope (JEOL) at 120 KV (negative staining) and 200 KV (ultrathin sections),
8 respectively. Images were recorded using a Megaview III CCD camera (Olympus SIS).

9 ***Bioinformatics***

10 All Influenza A M2 sequences deposited at www.ncbi.nlm.nih.gov were downloaded on 5 May
11 2011 in Fasta format and stored in one text file. 18,477 sequences with a length of at least 40
12 amino acids and including residue 50 were considered for further analysis. The sequences were
13 randomly split up into flat files containing 10,000 sequences each in order to speed up the
14 generation of multiple sequence alignments using ClustalW (Thompson *et al.*, 2002). The
15 multiple alignments comprising 10,000 sequences were concatenated into one single Fasta
16 sequence file and further processed with custom Perl scripts and Bioperl modules (Stajich *et al.*,
17 2002). The CRAC motif (L/V-X₁₋₅-Y-X₁₋₅-R/K) was extracted using Perl's regular expression
18 method.

19

20 **Acknowledgements**

21 We thank Robert Webster (St Jude Children's Research Hospital, Memphis, TN, USA) for
22 influenza virus expression plasmids, Hans-Dieter Klenk (Philipps-Universität Marburg,
23 Germany) for fowl plague virus antiserum, Elke Krüger (Charité, Berlin, Germany) for providing
24 A549 and MRC-5 cells, and Andrea Zoehner (RKI Berlin) for excellent technical assistance. The
25 German research foundation (DFG) is acknowledged for funding (SFB 740 TP C3, and SPP 1175).

26

1 **References**

2 **Castrucci, M. R., Hughes, M., Calzoletti, L., Donatelli, I., Wells, K., Takada, A. & Kawaoka, Y.**
3 **(1997).** The cysteine residues of the M2 protein are not required for influenza A virus
4 replication. *Virology* **238**, 128-134.

5 **Charollais, J. & Van Der Goot, F. G. (2009).** Palmitoylation of membrane proteins (Review).
6 *Mol Membr Biol* **26**, 55-66.

7 **Chen, B. J., Leser, G. P., Jackson, D. & Lamb, R. A. (2008).** The influenza virus M2 protein
8 cytoplasmic tail interacts with the M1 protein and influences virus assembly at the site of
9 virus budding. *J Virol* **82**, 10059-10070.

10 **Eisenberg, D., Weiss, R. M. & Terwilliger, T. C. (1984).** The hydrophobic moment detects
11 periodicity in protein hydrophobicity. *Proc Natl Acad Sci U S A* **81**, 140-144.

12 **Engel, S., Scolari, S., Thaa, B., Krebs, N., Korte, T., Herrmann, A. & Veit, M. (2010).** FLIM-
13 FRET and FRAP reveal association of influenza virus haemagglutinin with membrane
14 rafts. *Biochem J* **425**, 567-573.

15 **Grantham, M. L., Wu, W. H., Lalime, E. N., Lorenzo, M. E., Klein, S. L. & Pekosz, A. (2009).**
16 Palmitoylation of the influenza A virus M2 protein is not required for virus replication in
17 vitro but contributes to virus virulence. *J Virol* **83**, 8655-8661.

18 **Hess, S. T., Kumar, M., Verma, A., Farrington, J., Kenworthy, A. & Zimmerberg, J. (2005).**
19 Quantitative electron microscopy and fluorescence spectroscopy of the membrane
20 distribution of influenza hemagglutinin. *J Cell Biol* **169**, 965-976.

21 **Hoffmann, E., Neumann, G., Kawaoka, Y., Hobom, G. & Webster, R. G. (2000).** A DNA
22 transfection system for generation of influenza A virus from eight plasmids. *Proc Natl*
23 *Acad Sci U S A* **97**, 6108-6113.

24 **Jacobs, J. P., Jones, C. M. & Baille, J. P. (1970).** Characteristics of a human diploid cell
25 designated MRC-5. *Nature* **227**, 168-170.

26 **Lamb, R. A., Zebedee, S. L. & Richardson, C. D. (1985).** Influenza virus M2 protein is an
27 integral membrane protein expressed on the infected-cell surface. *Cell* **40**, 627-633.

28 **Leser, G. P. & Lamb, R. A. (2005).** Influenza virus assembly and budding in raft-derived
29 microdomains: a quantitative analysis of the surface distribution of HA, NA and M2
30 proteins. *Virology* **342**, 215-227.

31 **McCown, M. F. & Pekosz, A. (2006).** Distinct domains of the influenza a virus M2 protein
32 cytoplasmic tail mediate binding to the M1 protein and facilitate infectious virus
33 production. *J Virol* **80**, 8178-8189.

34 **Morozova, D. & Weiss, M. (2010).** On the role of acylation of transmembrane proteins. *Biophys*
35 *J* **98**, 800-804.

1 **Murata, M., Peranen, J., Schreiner, R., Wieland, F., Kurzchalia, T. V. & Simons, K. (1995).**
2 VIP21/caveolin is a cholesterol-binding protein. *Proc Natl Acad Sci U S A* **92**, 10339-
3 10343.

4 **Nayak, D. P., Balogun, R. A., Yamada, H., Zhou, Z. H. & Barman, S. (2009).** Influenza virus
5 morphogenesis and budding. *Virus Res* **143**, 147-161.

6 **Nguyen, P. A., Soto, C. S., Polishchuk, A., Caputo, G. A., Tatko, C. D., Ma, C., Ohigashi, Y., Pinto,
7 L. H., DeGrado, W. F. & Howard, K. P. (2008).** pH-induced conformational change of the
8 influenza M2 protein C-terminal domain. *Biochemistry* **47**, 9934-9936.

9 **Rossman, J. S., Jing, X., Leser, G. P., Balannik, V., Pinto, L. H. & Lamb, R. A. (2010a).** Influenza
10 virus m2 ion channel protein is necessary for filamentous virion formation. *J Virol* **84**,
11 5078-5088.

12 **Rossman, J. S., Jing, X., Leser, G. P. & Lamb, R. A. (2010b).** Influenza virus M2 protein mediates
13 ESCRT-independent membrane scission. *Cell* **142**, 902-913.

14 **Rossman, J. S. & Lamb, R. A. (2011).** Influenza virus assembly and budding. *Virology* **411**, 229-
15 236.

16 **Scheiffele, P., Roth, M. G. & Simons, K. (1997).** Interaction of influenza virus haemagglutinin
17 with sphingolipid-cholesterol membrane domains via its transmembrane domain. *EMBO*
18 *J* **16**, 5501-5508.

19 **Schroeder, C. (2010).** Cholesterol-binding viral proteins in virus entry and morphogenesis.
20 *Subcell Biochem* **51**, 77-108.

21 **Schroeder, C., Heider, H., Moncke-Buchner, E. & Lin, T. I. (2005).** The influenza virus ion
22 channel and maturation cofactor M2 is a cholesterol-binding protein. *Eur Biophys J* **34**,
23 52-66.

24 **Scolari, S., Engel, S., Krebs, N., Plazzo, A. P., De Almeida, R. F., Prieto, M., Veit, M. &
25 Herrmann, A. (2009).** Lateral distribution of the transmembrane domain of influenza
26 virus hemagglutinin revealed by time-resolved fluorescence imaging. *J Biol Chem* **284**,
27 15708-15716.

28 **Sharma, M., Yi, M., Dong, H., Qin, H., Peterson, E., Busath, D. D., Zhou, H. X. & Cross, T. A.
29 (2010).** Insight into the mechanism of the influenza A proton channel from a structure in
30 a lipid bilayer. *Science* **330**, 509-512.

31 **Stewart, S. M. & Pekosz, A. (2011).** Mutations in the membrane proximal region of the
32 influenza A virus M2 protein cytoplasmic tail have modest effects on virus replication. *J*
33 *Virol.*

34 **Stewart, S. M., Wu, W. H., Lalime, E. N. & Pekosz, A. (2010).** The cholesterol
35 recognition/interaction amino acid consensus motif of the influenza A virus M2 protein
36 is not required for virus replication but contributes to virulence. *Virology* **405**, 530-538.

- 1 **Sugrue, R. J., Belshe, R. B. & Hay, A. J. (1990).** Palmitoylation of the influenza A virus M2
2 protein. *Virology* **179**, 51-56.
- 3 **Takeda, M., Pekosz, A., Shuck, K., Pinto, L. H. & Lamb, R. A. (2002).** Influenza a virus M2 ion
4 channel activity is essential for efficient replication in tissue culture. *J Virol* **76**, 1391-
5 1399.
- 6 **Thaa, B., Herrmann, A. & Veit, M. (2010).** Intrinsic cytoskeleton-dependent clustering of
7 influenza virus M2 protein with hemagglutinin assessed by FLIM-FRET. *J Virol* **84**,
8 12445-12449.
- 9 **Thaa, B., Levental, I., Herrmann, A. & Veit, M. (2011).** Intrinsic membrane association of the
10 cytoplasmic tail of influenza virus M2 protein and lateral membrane sorting regulated by
11 cholesterol binding and palmitoylation. *Biochem J* **437**, 389-397.
- 12 **Veit, M., Klenk, H. D., Kendal, A. & Rott, R. (1991).** The M2 protein of influenza A virus is
13 acylated. *J Gen Virol* **72 (Pt 6)**, 1461-1465.
- 14 **Veit, M., Ponimaskin, E. & Schmidt, M. F. (2008).** Analysis of S-acylation of proteins. *Methods*
15 *Mol Biol* **446**, 163-182.
- 16 **Veit, M. & Thaa, B. (2011).** Association of Influenza Virus Proteins with Membrane Rafts.
17 *Advances in Virology* doi:10.1155/2011/370606.
- 18 **Zebedee, S. L. & Lamb, R. A. (1988).** Influenza A virus M2 protein: monoclonal antibody
19 restriction of virus growth and detection of M2 in virions. *J Virol* **62**, 2762-2772.
- 20 **Zhang, J., Pekosz, A. & Lamb, R. A. (2000).** Influenza virus assembly and lipid raft
21 microdomains: a role for the cytoplasmic tails of the spike glycoproteins. *J Virol* **74**,
22 4634-4644.
- 23 **Zhirnov, O. P., Konakova, T. E., Garten, W. & Klenk, H. (1999).** Caspase-dependent N-terminal
24 cleavage of influenza virus nucleocapsid protein in infected cells. *J Virol* **73**, 10158-
25 10163.
- 26
27
28

1 Figure Legends

2

3 **Figure 1:** (a) Topology sketch of M2, orientation of transmembrane domain and amphiphilic
4 helix in the cytoplasmic tail according to NMR structural analysis (Sharma *et al.*, 2010). The
5 acylation site (C50) and the tyrosines (Y52, Y57) in the cholesterol recognition/interaction
6 amino acid consensus (CRAC) motifs are indicated. (b), helical wheel plot (axial view) of the
7 amphiphilic helix (residues 46–61) of M2 from Influenza A/WSN/33 generated with Heliquest
8 (heliquest.ipmc.cnrs.fr), orientation according to NMR structure (Sharma *et al.*, 2010).
9 Hydrophobic residues in light grey, polar residues in dark grey. Arrows mark the residues
10 substituted in this study. (c–e), helical wheel plot of M2's amphiphilic helix indicating the
11 residues changed in the studies of others (c: (Grantham *et al.*, 2009), d: (Stewart *et al.*, 2010), e:
12 (Rossman *et al.*, 2010a)), virus strain: WSN (c, d)/Udorn (e, amino acid differences compared
13 with WSN labelled in *italics*). See text for details.

14

15 **Figure 2:** Growth of recombinant influenza viruses (WSN strain) with mutations in M2. (a),
16 representative plaque assays of WSN wildtype (top left) and carrying the indicated mutations.
17 (b–d), growth curves. MDCK II (b), A549 (c) or MRC-5 (d) cells were infected with the indicated
18 virus at MOI = 0.01, cell culture supernatants were harvested after the indicated times and
19 tested for infectious titres by plaque assay. The experiments were done in triplicate and are
20 displayed as mean \pm standard deviation. The titre reduction of WSN M2: Y52S, Y57S was
21 observed in each experiment. Non-discernible error bars are smaller than the respective data
22 point symbol.

23

24 **Figure 3:** Characterisation of WSN wildtype and mutants thereof by transmission electron
25 microscopy. (a), representative negative stain images of the indicated virus harvested from the
26 supernatant of infected MDCK cells. Scale bar, 200 nm. (b), representative ultrathin sections of
27 MDCK cells infected with WSN M2: Y52S, Y57S. Scale bar, 200 nm.

28

29 **Figure 4:** Determination of viral protein content. (a), Radioactively labelled WSN (wildtype and
30 indicated mutants) were generated by infection of MDCK cells in the presence of [³⁵S]-
31 methionine/-cysteine, pelleted from the cell culture supernatant and subjected to SDS-PAGE and
32 fluorography. Band intensities from this and three other experiments were quantified by
33 densitometry on scanned films. The mean HA/M1 ratios (normalised to wildtype) are displayed
34 below each lane. (b), M2 and M1 were detected by Western blot. The indicated mean M2 content
35 in the viruses (relative to M1, normalised to wildtype) was determined from three experiments.

1 The position of the viral proteins is indicated on the right-hand side, molecular weight marker
2 (kDa) on the left-hand side.

3

4 **Figure 5:** Competitive growth of WSN wildtype and WSN mutant M2: Y52S, Y57S. (a),
5 sequencing chromatograms of copy-DNA of WSN wt (left-hand side) and WSN mut (right-hand
6 side). (b and c), 2.4×10^6 MDCK cells were infected with 12,000 plaque-forming units (pfu) of
7 WSN wt and mut at a ratio of 1:1 (b) or 1:5 (c), supernatants were collected at the indicated
8 times post-infection, viral RNA was isolated, subjected to RT-PCR and sequenced. Nucleotide
9 exchanges are indicated with black arrows.

10

1 Tables

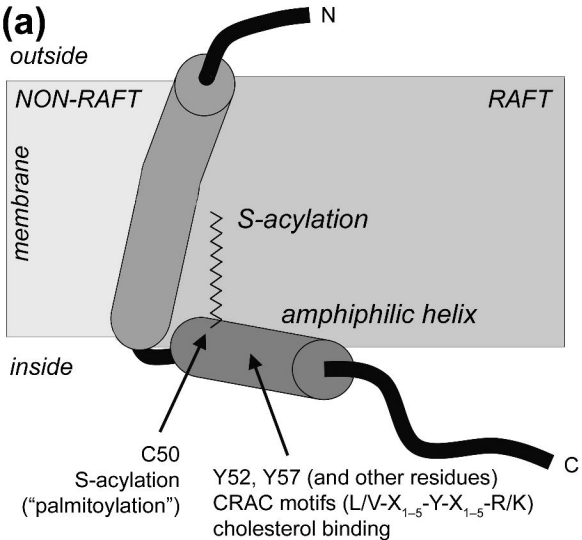
	C50	S50	F50	Y50	others	<i>total</i>
+CRAC	15,522 (84.0 %)	2,035 (11.0 %)	407 (2.2 %)	92 (0.5 %)	6 (0.0 %)	18,062 (97.8 %)
-CRAC	357 (1.9 %)	58 (0.3 %)	0 (0.0 %)	0 (0.0 %)	0 (0.0 %)	415 (2.2 %)
<i>total</i>	15,879 (85.9 %)	2,093 (11.3 %)	407 (2.2 %)	92 (0.5 %)	6 (0.0 %)	18,477 (100.0 %)

3
4 **Table 1:** Numbers of influenza A M2 sequences retrieved from www.ncbi.nlm.nih.gov, grouped
5 according to the identity of residue 50 and to the presence or absence of CRAC motifs.

mutation	sequence (residues 46–61)	CRAC	hydrophobic moment μ_H	impaired virus growth	ref.
<i>WSN strain</i>					
wt	LFFKCIYRRFKYGLKR	+	0.422		
R54F	LFFKCIYR F FKYGLKR	+	0.492		*
L46A, Y52A, R54A	A FFKCI A R A FKYGLKR	-	0.523		*
C50S	LFFK S IYRRFKYGLKR	+	0.475		†, §
Y52S, Y57S	LFFKCI S RRFK S GLKR	-	0.461		§
C50S, Y52S, Y57S	LFFK S I S RRFK S GLKR	-	0.510		§
<i>Udorn strain</i>					
wt	LFFKCIYRFFEHGLKR	-	0.502		
F54R	LFFKCIYR R FEHGLKR	+	0.451		*
C50S	LFFK S IYRFFEHGLKR	-	0.533		†, ‡
F47A	L AFKCIYRFFEHGLKR	-	0.439		‡
F48A	L F A KCIYRFFEHGLKR	-	0.457		‡
I51A	LFFK C A A YRFFEHGLKR	-	0.409		‡
Y52A	LFFKCI A RFFEHGLKR	-	0.508		‡
F55A	LFFKCIYR F A EHGLKR	-	0.431		‡
F47A, F48A, I51A, Y52A, F55A	L A A K C A A R F A EHGLKR	-	0.244	yes	‡

8
9 **Table 2:** Amphiphilicity of the helix formed by residues 46–61 in the cytoplasmic tail of M2 and
10 different mutants thereof, studied in the context of the virus in this study and the indicated
11 references. The hydrophobic moment μ_H is displayed as calculated with heliquiest.ipmc.cnrs.fr.
12 The presence or absence of CRAC motifs is indicated. References: *, (Stewart *et al.*, 2010); †,
13 (Grantham *et al.*, 2009); ‡, (Rossman *et al.*, 2010a), §, this work.

14



(b) *M2 of Influenza A/WSN/33*

